IEEE International Symposium on Industrial Electronics (ISIE 2009)
Seoul Olympic Parktel, Seoul, Korea July 5-8, 2009

Comparisons of Six-Step Square-Wave PWMs in Ultra-Low-Power SOC Integration

Hung-Chi Chen (IEEE Member), Tzu-Yang Tsai, *Chih-Kai Huang,
Department of Electrical and Control Engineering,
National Chiao Tung University, HsinChu, Taiwan.
*Industrial Technology Research Institute, HsinChu, Taiwan.
hcchen@cn.nctu.edu.tw

***Abstract*- It is well-known that ultra-low-power three-phase elements, such as ultra-small-size permanent-magnet brushless motor drivers, have been widely used in the consumer products. In order to reduce the cost, size and power consumption of products, it is necessary to integrate the system functions with square-wave PWM (SWPWM) driver in the system-on-chip (SOC) implementation. It follows that, the driver loss and loss distribution are the main challenges in the integration of ultra-low-power SWPWM driver where the driver loss include conducting loss, switching loss and gate driving loss, where the last one is often neglected in other low-, medium- and high-power drivers. On the other hand, there are 16 types and 64 types in 120-degree SWPWM and 180-degree SWPWM, respectively, and the resulting driver loss and loss distribution differ from each other. This paper studies the driver loss and loss distributions of all SWPWM types in detail. The result shows that SWPWM type-01_01, type-10_10 and type-010_010 are the recommended types in the SOC integration of ultra-low-power SWPWM driver.**

I. INTRODUCTION

In many consumer equipments such as data-storage equipments and audio-visual equipments, small-sized permanent magnet brushless motor had been widely used [1-2]. To control the small-sized motor, motor driver composed of switching signal generating circuits and power circuits are expected to be integrated with the other function circuits on the same chip – system-on-chip (SOC). As technology scales, power consumption and thermal effects have become challenges for SOC designers. The rising on-chip temperature can have negative impacts on SOC performance [3].

A linear motor drive system is widely used due to its advantage of smooth rotation and low rate of changed current in the motor coils. However, like linear power supply, the linear motor driver system suffers from a series disadvantage of large power consumption in the driver circuit. To reduce the power consumption, more and more switch-mode drive systems are used to control the brushless spindle motors in electronic equipments [2].

The losses of three-phase SWPWM driver can be divided into conducting loss, switching loss and gate driving loss. The first two losses are highly dependent on the electrical characteristics of used power switches, but their distributions are different from various SWPWM types [4].

In the practical circuit, voltage transition at any node would contribute to energy loss due to the load capacitance. Therefore, even though no load is connected to the inverter output, the gate driving loss exists in the SWPWM drivers. Compared to the switching loss and conduction loss, the relatively small gate driving loss is often neglected in most SWPWM drivers. But for an ultra-low-power SWPWM driver, the gate driving loss occupies significant part of the driver loss.

This paper studies all existing six-step square-wave PWM (SWPWM) schemes from the driver loss and loss distribution. Then, we choose the best SWPWM types as the recommended ones to be applied to SOC integration. To the author's best knowledge, all SWPWM schemes have not yet been studied in detail and first listed in this paper. The provided experimental results also show the recommended types.

II. SIX-SWITCH INVERTER

The simplified schematic of three-phase six-switch voltage source inverter (VSI) is shown in Fig. 1 where three-phase balanced resistances R are connected to it. The supply voltage magnitude of individual gate driving circuit is V_{GS}. The input capacitances C_{iss} of power switches are also plotted in order to represent the gate driving loss due to the transition of gate voltage.

By using KCL, the switch currents i_{T1} and i_{T4} can represented in terms of the output current i_a as follows:

$$i_{T1} = \begin{cases} i_a, & when\ \ i_a > 0 \\ 0, & when\ \ i_a \le 0 \end{cases} \quad (1)$$

$$i_{T4} = \begin{cases} 0, & when\ \ i_a \ge 0 \\ -i_a, & when\ \ i_a < 0 \end{cases} \quad (2)$$

For square-wave modulations (SWM), the simplest way to adjust the magnitude of output voltage is changing the dc-link voltage V_d. However, in most cases, the dc-link voltage is not controllable. Therefore, in the applications of uncontrolled dc-link-voltage, SWM should be work together with pulse width modulation (PWM) to become square-wave pulse-width-modulation (SWPWM) in order to generate the controllable output voltage. It follows that the switching signals G_{T1} ~ G_{T6} may keep discontinuous "on" with duty ratio D between any two commutation instants.

Due to the input capacitance C_{iss} of power switch, any transition (0-to-V_{GS} as shown in Fig. 1) in the switch gate voltage would consume some power even when the power

978-1-4244-4349-9/09/$25.00 ©2009 IEEE

switch does not conduct any current. Depending on the various gate signal generating schemes, the output transition rate can be slower than the PWM frequency f_{PWM}. To better represent this behavior, the effective PWM transition rate $\alpha_{PWM,x}$ experienced per fundamental cycle will be introduced. Then, the average gate driving loss due to input capacitance C_{iss} becomes

$$P_{G,Tx} = C_{iss} V_{GS}^2 f_{PWM} \alpha_{PWM,x} \tag{3}$$

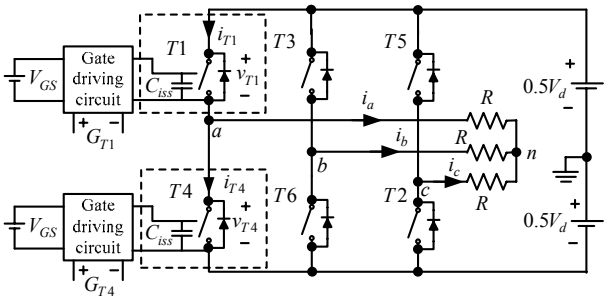

Fig. 1. Simplified schematic of three-phase six-switch VSI.

The switching loss equally occurring in the upper switch and the lower switch is better than the switching loss is poured to either upper switch or the lower switch. In order to represent the loss distribution, the gate driving loss distribution factor $F_{G,TD}$ and the switching loss distribution factor $F_{S,TD}$ are defined in the followings,

$$F_{G,TD} = \frac{\left|P_{G,T1} - P_{G,T4}\right|}{P_{G,T1} + P_{G,T4}} \tag{4}$$

$$F_{S,TD} = \frac{\left|P_{S,T1} - P_{S,T4}\right|}{P_{S,T1} + P_{S,T4}} \tag{5}$$

III. SIX-STEP 120° SWPWM

In the common 120° SWPWM, each switch conducts for 120°. It follows that there are six commutations in each periodic cycle. We can find that at any instant, only two switches conducts. Therefore, a 60° dead-time exists between the switching signals of upper switch and the lower switch of the same leg, which avoids the occurrence of short of dc voltage

It is clear that 120° conduction scheme in each switch is composed of two neighbor conduction patterns. There are total four conduction patterns involved in the two switching signals of each leg. In order to apply SWPWM to adjust the output voltage, the conduction state in each conduction pattern is not always continuous "on". It may be either continuous "on" or discontinuous "on" (i.e. PWM "on"). Consequently, it follows that there are $2^4 = 16$ possible types in 120° SWPWM. The definition of 120° SWPWM scheme is defined as type-$U_1U_2\_L_1L_2$ where

$$U_m = \begin{cases} 0, \text{ when } m\text{th switching signal of upper switch is continuous "on"} \\ 1, \text{ when } m\text{th switching signal of upper switch is PWM "on"} \end{cases} \tag{6}$$

$$L_m = \begin{cases} 0, \text{ when } m\text{th switching signal of upper switch is continuous "on"} \\ 1, \text{ when } m\text{th switching signal of upper switch is PWM "on"} \end{cases} \tag{7}$$

By following (6)-(7), the common 120° SWM can be seen as the type of 00_00 whose switching signals are always continuous "on". For type 01_01, all switching signals, the output voltage and current waveforms are plotted in Fig. 2 [5]. We can find that each switching signal holds the voltage level at the first 60° period and then alternates for the next 60° period.

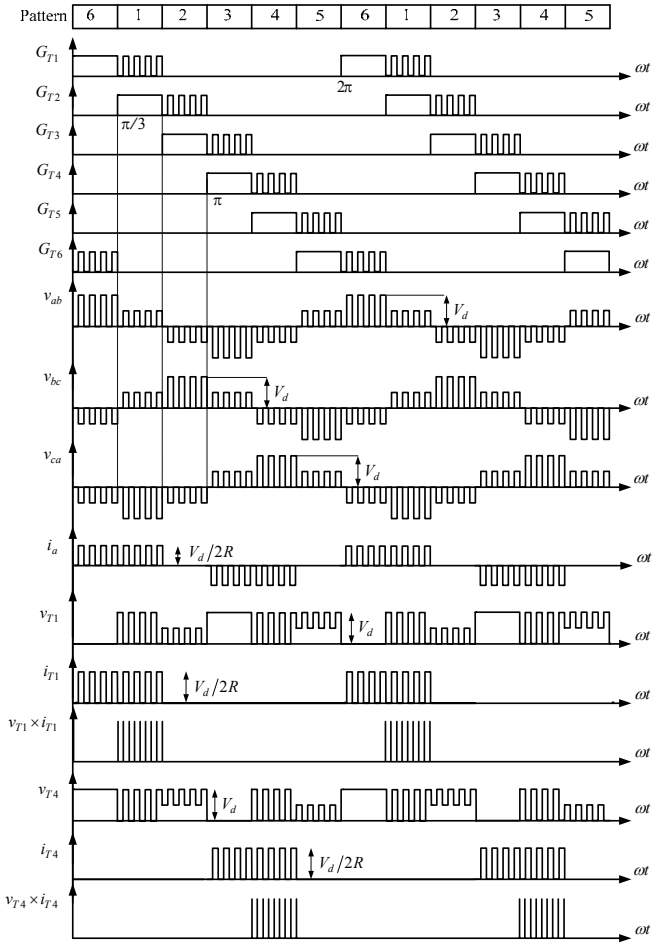

Fig. 2. Illustrated waveforms of type 01_01 [5].

The output voltage $v_{ab}^{120°}$ as shown in Fig. 2 can be expressed in Fourier series as:

$$v_{ab}^{120°}(t) = \sum_{h=1}^{\infty}\left(\frac{4}{h\pi} D V_d \sin^2\left(\frac{h\pi}{2}\right)\cos^2\left(\frac{h\pi}{6}\right)\sin h\left(2\pi f_1 t + \frac{\pi}{3}\right)\right)$$
$$h \in \text{positive integer } N \tag{8}$$

where f_1 is the fundamental frequency in *Hz*, D is the PWM duty ratio. All the even and triple harmonics (3, 9, 15 ...) in

$v_{ab}^{120^\circ}$ are zeros. By calculation, the fundamental component $V_{ab,1}^{120^\circ}$ of output voltage $v_{ab}^{120^\circ}$ can be expressed as:

$$V_{ab,1}^{120^\circ} = \frac{3}{\pi} D V_d \tag{9}$$

Obviously, the fundamental output voltage in 120° SWPWM type 01_01 can be linearly controlled from near zero to its maximum value $3V_d/\pi$ by adjusting the duty ratio D. However, not all 120° SWPWM types possess the same linear equation in (9). Fig. 3 plots the output voltage waveforms of all 120° SWPWM types. Obviously, in types 00_00, 00_01, 00_10, 01_00, 01_10, 10_00, and 10_01, their fundamental output voltages are not always linear with duty ratio D. Additionally, the other types 00_11, 01_01, 01_11, 10_10, 10_11, 11_00, 11_01, 11_10 and 11_11 possess the same controllable output voltage as (8) and they are named linear 120° SWPWM schemes.

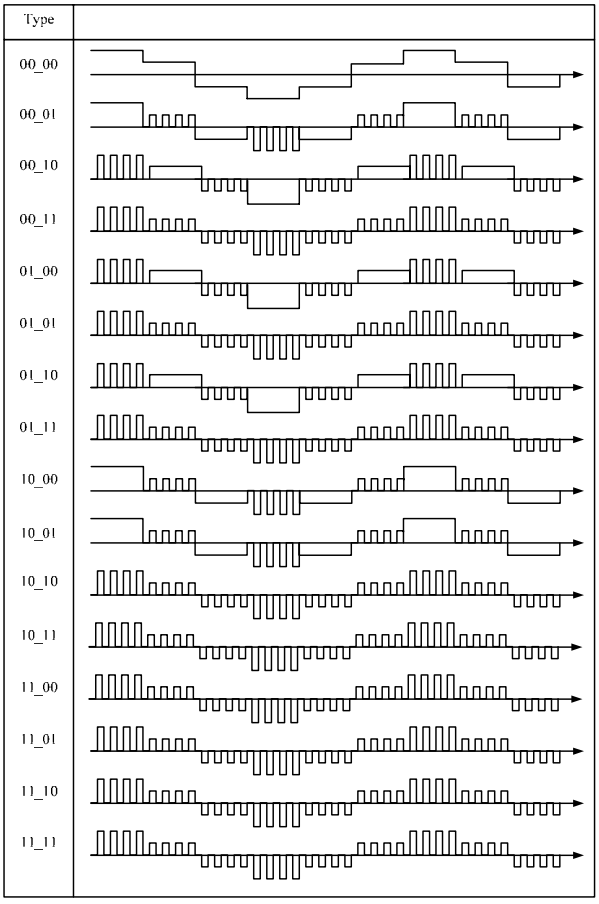

Fig. 3. The output voltage $v_{ab}^{120^\circ}$ of all 120° SWPWM schemes.

According to (8), the h th-order harmonic voltage can be expressed as:

$$V_{ab,h}^{120^\circ} = \frac{1}{h}\frac{3}{\pi} D V_d = \frac{V_{ab,1}^{120^\circ}}{h} \qquad h = 6r \pm 1 \text{; integer } r \geq 1 \tag{10}$$

Equation (10) shows that nonzero hth-order harmonic component $V_{ab,h}^{120^\circ}$ increases with PWM duty ratio D and the fundamental voltage $V_{ab,1}^{120^\circ}$. However, (10) holds only when its harmonic order h is significantly lower than the frequency modulation ratio m_f. As listed in Table II, the other harmonics centered around the PWM frequency f_{PWM} and its multiples do not increase with duty ratio D.

Table I. Harmonic components in linear 120° and 180° SWPWM

h \ D	0.1	0.3	0.5	0.7	0.9
1	0.1	0.3	0.5	0.7	0.9
5	0.02	0.06	0.1	0.14	0.18
7	0.0142	0.0428	0.0714	0.1	0.1285
11	0.0091	0.0273	0.0455	0.0636	0.0818
13	0.0077	0.0231	0.0385	0.0538	0.0692
$m_f \pm 1$	0.0945	0.2500	0.3106	0.0265	0.1013
$m_f \pm 3$	0.0006	0.0013	0.0018	0.0010	0.0007
$m_f \pm 5$	0.0191	0.0526	0.0704	0.0593	0.0113
$2m_f \pm 1$	0.0924	0.1516	0.0061	0.1557	0.0875
$2m_f \pm 3$	0.0006	0.0011	0.0002	0.0005	0.0006
$2m_f \pm 5$	0.0176	0.0353	0.0062	0.0349	0.0131

Note: The value tabulated in $V_{ab,h}^{120^\circ} \Big/ \frac{3}{\pi} V_d$, $V_{ab,h}^{180^\circ} \Big/ \frac{2\sqrt{3}}{\pi} V_d$.

Moreover, due to the input capacitance C_{iss} of the power switch, the more time the switching signals take to change for PWM, the more driving loss the circuit can yield. The effective PWM transition rate of upper switching signals G_{T1}, G_{T3}, G_{T5} and lower switching signals G_{T2}, G_{T4}, G_{T6} are defined as

$$\alpha_{PWM,1}^{120^\circ} = \alpha_{PWM,3}^{120^\circ} = \alpha_{PWM,5}^{120^\circ} = \frac{1}{6}\sum_{i=1}^{2} U_i \tag{11}$$

$$\alpha_{PWM,4}^{120^\circ} = \alpha_{PWM,6}^{120^\circ} = \alpha_{PWM,2}^{120^\circ} = \frac{1}{6}\sum_{i=1}^{2} L_i \tag{12}$$

where U_i and L_i had been defined in (6)-(7), respectively. Then the total driving loss $P_G^{120^\circ}$ is

$$\begin{aligned} P_G^{120^\circ} &= \sum_{x=1}^{6} P_{G,Tx}^{120^\circ} = C_{iss} V_{GS}^2 f_{PWM} \left(\sum_{x=1}^{6} \alpha_{PWM,x}\right) \\ &= C_{iss} V_{GS}^2 f_{PWM} \frac{1}{2}\left(\sum_{i=1}^{2} U_i + \sum_{i=1}^{2} L_i\right) \end{aligned} \tag{11}$$

It follows that the effective PWM transition rate of 120° SWPWM type-$U_1U_2\_L_1L_2$ can be represented by

$$\alpha_{PWM}^{120^\circ} = \frac{1}{2}\left(\sum_{i=1}^{2} U_i + \sum_{i=1}^{2} L_i\right) \tag{12}$$

According to the value $\alpha_{PWM}^{120^\circ}$, all linear 120° SWPWM schemes can be classified into Table II. The higher value $\alpha_{PWM}^{120^\circ}$ is, the higher driving loss is. It means that there are four 120° SWPWM types 01_01 [5], 10_10 [6], 11_00 [4, 7-8], 00_11 [9] with minimum value $\alpha_{PWM}^{120^\circ} = 1$. In fact, these four types are often found in the literatures [4-9]. But the other types with higher value $\alpha_{PWM}^{120^\circ}$ had not yet found in any literatures.

Additionally, it is noted that based on the thermal consideration, the loss distribution in upper switch and the

lower switch is another important issue. From the voltages and the currents of the switches as shown in Fig. 2, we can find that `in type-10_10, the switching loss $P_{S,T1}$ and $P_{S,T4}$ are equal to each other.

Table II. Loss and distribution of various linear 120° SWPWM types

type	$\alpha_{PWM}^{120^\circ}$	$F_{G,TD}^{120^\circ}$	$F_{S,TD}^{120^\circ}$
01_01	**1**	**0**	**0**
10_10	**1**	**0**	**0**
00_11	1	1	1
11_00	1	1	1
01_11	1.5	0.333	0.5
11_01	1.5	0.333	0.5
10_11	1.5	0.333	0.5
11_10	1.5	0.333	0.5
11_11	2	0	0

Not all the linear 120° SWPWM types possess good loss distribution. The loss distribution factors $F_{G,TD}$ and $F_{S,TD}$ defined in (4) and (5) of all linear 120° SWPWM types can be found in Table III. Zero loss distribution factors means that the loss distribution is even. It follows that no hot spot can be found in the main power circuit of ultra-small-size SWPWM drivers by using the linear 120° SWPWM types with zero loss distribution factors. Therefore, it follows that type-01_01 and type-10_10 are the best types of 120° SWPWM.

IV. SIX-STEP 180° SWPWM

In the common 180° SWM, each switch conducts for 180°. Like 120° SWPWM, there are also six commutations per periodic cycle in 180° SWPWM and thus, there are six conduction patterns. The conduction of the upper switch closely follows the conduction of the lower switch, and vice versa. Therefore, in practice, some blanking time must be included in their switching signals to avoid the short circuits of the dc bus due to the simultaneous conduction of the lower and upper switches.

180° conduction in each switch is composed of three neighbor conduction patterns. There are total six conduction patterns involved in each leg. In order to apply SWPWM to adjust the output voltage, the conduction state in each conduction pattern is not always continuous "on". It may be either continuous "on" or discontinuous "on" (i.e. PWM "on"). Consequently, there are $2^6 = 64$ possible types in 180° SWPWM. Each 180° SWPWM is represented as type-$U_1U_2U_3\_L_1L_2L_3$ where the definitions of U_m and L_m can be found in (6)-(7).

By following the above definition, the common 180° SWM can be seen as 180° SWPWM type-000_000 whose switching signals are always continuous "on". All switching signals for 180° SWPWM type-010_010 and the output voltages are plotted in Fig. 4.

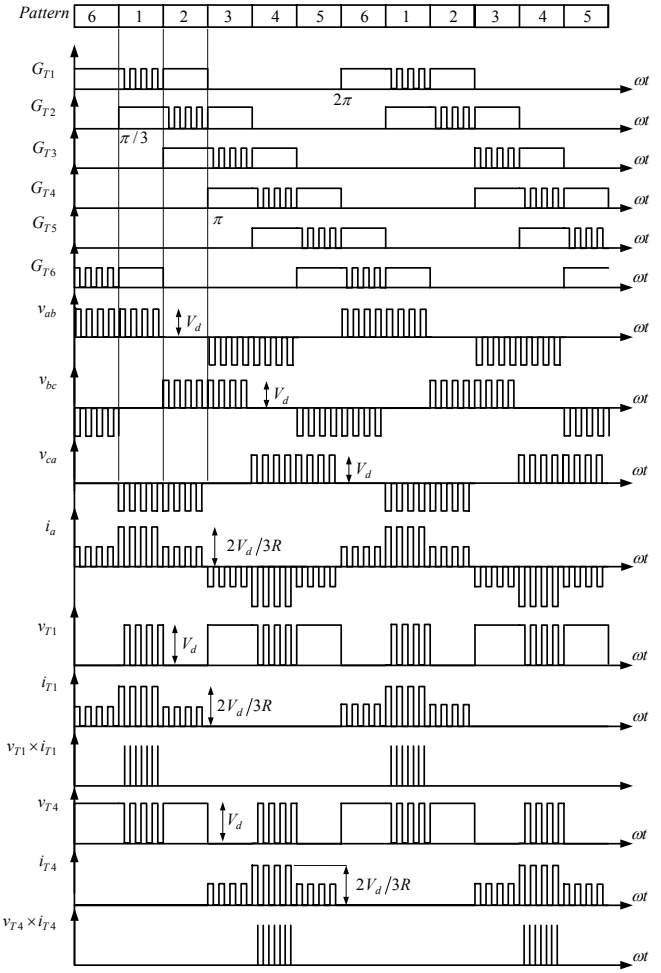

Fig. 4. Illustrated waveforms for type-010_010.

We can find that in Fig. 4, each switch conducts continuously for 60°, then conducts discontinuously for the following 60° and conducts continuously for the remaining 60°. Because that the output voltage $v_{ab}^{180^\circ}$ can be expressed in Fourier series as:

$$v_{ab}^{180^\circ}(t) = \sum_{h=1}^{\infty} \frac{4DV_d}{h\pi} \sin\left(\frac{h\pi}{2}\right) \sin\left(\frac{h\pi}{3}\right) \sin h\left(\omega t + \frac{\pi}{6}\right)$$
$$h \in N > 0 \tag{13}$$

All the even and triple harmonics (3, 9, 15 ...) in $v_{ab}^{180^\circ}$ are zeros. By calculation, the fundamental component $V_{ab,1}^{180^\circ}$ of output voltage $v_{ab}^{180^\circ}$ can be expressed as:

$$V_{ab,1}^{180^\circ} = \frac{2\sqrt{3}}{\pi} DV_d \tag{14}$$

Obviously, the fundamental output voltage $V_{ab,1}^{180^\circ}$ can be easily controlled from near zero to maximum output voltage

$2\sqrt{3}V_d/\pi$ by adjusting the duty ratio *D*. According to (13), the h th-order harmonic voltage can be expressed as:

$$V_{ab,h}^{180^\circ} = \frac{1}{h}\frac{2\sqrt{3}}{\pi}DV_d = \frac{V_{ab,1}^{180^\circ}}{h} \quad h = 6r \pm 1 \text{; integer } r \geq 1 \qquad (15)$$

However, not all 180° SWPWM types possess the controllable fundamental voltage as (14). Table III tabulates the classification of various output voltage waveforms for all 180° SWPWM types. Obviously, according to Table III, only 25 types possess the controllable fundamental voltage, i.e. linear modulation.

Equation (15) shows that nonzero *h*th-order harmonic component increases with PWM duty ratio *D* and the fundamental voltage $V_{ab,1}^{180^\circ}$ and, however, it holds only when the harmonic order *h* is significantly lower than the frequency modulation ratio m_f. The voltage harmonics $V_{ab,h}^{180^\circ}$ in linear 180° SWPWM types possess the same proportionality as (10) in linear 120° SWPWM schemes. Therefore, the voltage harmonics of linear 180° SWPWM types can also be found from the same Table I as for linear 120° SWPWM schemes.

Table III Classification of output voltage $v_{ab}^{180^\circ}$ for all 180° SWPWM types

Types	Output voltage waveform
000_000	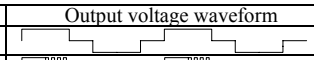
000_001, 000_100, 001_000, 100_000	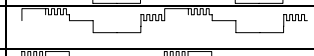
000_010, 000_101, 001_010, 100_010, 101_000, 101_010, 010_000, 010_001, 010_100, 010_101	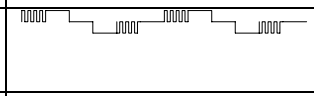
000_011, 000_110, 001_101, 001_011, 001_110, 100_110, 101_100, 100_101, 101_110, 011_000, 011_001, 011_100, 011_101, 110_000, 110_001, 110_100, 110_101, 100_011, 101_001, 101_011	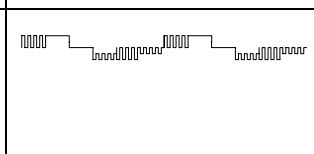
001_001, 100_100	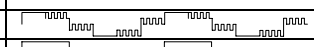
001_100, 100_001	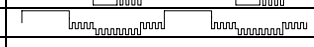
000_111, 001_111, 010_010, 010_011, 010_110, 010_111, 011_010, 011_011, 011_110, 011_111, 100_111, 101_101, 101_111, 110_010, 110_011, 110_110, 110_111, 111_000, 111_001, 111_010, 111_011, 111_100, 111_101, 111_110, 111_111[10]	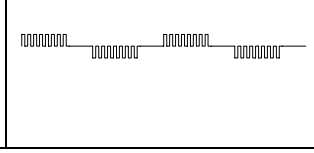

By following (12), the effective PWM transition rate of 180° SWPWM type-$U_1U_2U_3\_L_1L_2L_3$ can be represented by

$$\alpha_{PWM}^{180^\circ} = \frac{1}{2}\left(\sum_{i=1}^{3}U_i + \sum_{i=1}^{3}L_i\right) \qquad (16)$$

Then the total gate driving loss $P_G^{180^\circ}$ of 180° SWPWM type-$U_1U_2U_3\_L_1L_2L_3$ is

$$P_G^{180^\circ} = \sum_{x=1}^{6}P_{G,Tx}^{180^\circ} = C_{iss}V_{GS}^2 f_{PWM}\alpha_{PWM}^{180^\circ} \qquad (17)$$

The higher value $\alpha_{PWM}^{180^\circ}$ of 180° SWPWM type-$U_1U_2U_3\_L_1L_2L_3$ is, the higher driving loss of type-$U_1U_2U_3\_L_1L_2L_3$ is. According to effective PWM transition rate $\alpha_{PWM}^{180^\circ}$, all 25 linear 180° SWPWM types can be classified into Table IV. From Table IV, we can find that only type-010_010 has minimum value $\alpha_{PWM}^{180^\circ} = 1$.

However, based on the thermal consideration, the loss distribution in upper switch and the lower switch is another important issue. From the voltages and the currents of the switches as shown in Fig. 4, we can find that in type-010_010, the switching loss $P_{S,T1}$ and $P_{S,T4}$ are equal to each other.

For type-111_000, all the switching loss occurs only in the upper switch. Therefore, not all the linear 180° SWPWM types possess good loss distribution. The loss distribution factors $F_{G,TD}$ and $F_{S,TD}$ defined in (5) and (6) of all linear 180° SWPWM types can be found in Table IV. It follows that by using the linear 180° SWPWM with zero loss distribution factors, no hot spot due to SWPWM driver circuit can be expected in the driver circuit.

By considering the linear modulation in Table III and loss distribution in Table IV, we can find that only type-010_010 is the best selection of 180° SWPWM.

Table IV. Loss and distribution of various linear 180° SWPWM types

type	$\alpha_{PWM}^{180^\circ}$	$F_{G,TD}^{180^\circ}$	$F_{s,TD}^{180^\circ}$
010_010	**1**	**0**	**0**
000_111	1.5	1	1
010_011	1.5	0.333	0
010_110	1.5	0.333	0
011_010	1.5	0.333	0
101_111	1.5	0.333	0.5
110_010	1.5	0.333	0
111_000	1.5	1	1
001_111	2	0.5	1
010_111	2	0.5	0.5
011_011	2	0	0
011_110	2	0	0
100_111	2	0.5	1
101_101	2	0	0
110_011	2	0	0
110_110	2	0	0
111_001	2	0.5	1
111_010	2	0.5	0.5
111_100	2	0.5	1
011_111	2.5	0.25	0.5
110_111	2.5	0.25	0.5
111_011	2.5	0.25	0.5
111_101	2.5	0.25	0.5
111_110	2.5	0.25	0.5
111_111	3	0	0

V. EXPERIMENTAL RESULTS

As shown in Fig. 1, a MCU-based SWPWM inverter is implemented. The DC link voltage of the voltage source inverter is $V_{DC} = 150V$ and the used balanced load resistances are 100Ω. All the six-step SWPWM switching signals $G_{T1} \sim G_{T6}$ with blanking time are implemented in MCU.

A. 120° *SWPWM*

The experimental waveforms for 120° SWPWM type-01_01 and type-11_00 are plotted in Fig. 5, respectively. Compared Fig. 5 with Fig. 2, we can make sure that the illustrated waveforms are very close to the experimental results. Thus, the classification of effective PWM transition $\alpha_{PWM}^{120^\circ}$ and

loss distribution of gate driving loss $F_{G,TD}^{120°}$ in Table III are correct.

Due to the used six-switch power module, it is hard to measure the switch currents i_{T1} and i_{T4} directly. However, based on (1)-(2), the currents i_{T1} and i_{T4} can be synthesized from the inverter output current i_a. Therefore, the illustrated waveforms of products $v_{T1} \times i_{T1}$ and $v_{T4} \times i_{T4}$ in Fig. 2 and the following loss distribution factor $F_{S,TD}^{120°}$ in Table IV can be trusted. It follows that type-01_01 and type-10_10 with minimum effective PWM transition rate and even loss distribution are the best selection of 120° SWPWM.

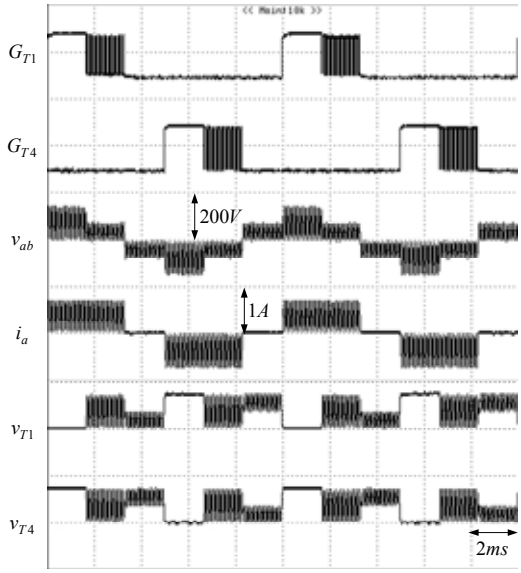

Fig. 5. Experimental waveforms for 120° SWPWM type-01_01.

B. 180° *SWPWM*

The experimental waveforms for 180° SWPWM type-010_010 are plotted in Fig. 6, respectively. Compared Fig. 6 with Fig. 4, we can also find that the illustrated waveforms are very close to the experimental results. Thus, the classification of effective PWM transition $\alpha_{PWM}^{180°}$ and loss distribution of gate driving loss $F_{G,TD}^{180°}$ in Table IV are correct.

The illustrated waveforms of products $v_{T1} \times i_{T1}$ and $v_{T4} \times i_{T4}$ in Fig. 4 and the switching loss distribution $F_{S,TD}^{180°}$ in Table IV also can be trusted. It demonstrates that type-010_010 is the best selection of 180° SWPWM.

VI. Conclusions

In order to integrate the ultra-small-power SWPWM drivers into SOC integration, we should minimize the gate driving driver loss, reduce temperature rise and eliminate possible hot spot in the SWPWM driver. With the common six-switch circuit topology, selection of recommended SWPWM types is an effective way to overcome the SOC challenges – power consumption and thermal balance. After the classification of linear modulation, effective PWM transition rate α_{PWM}, loss distribution factor and experimental demonstration, this paper recommends the following best SWPWM schemes for SOC design -- type 01_01 and 10_10 for 120° SWPWM and type 010_010 for 180° SWPWM.

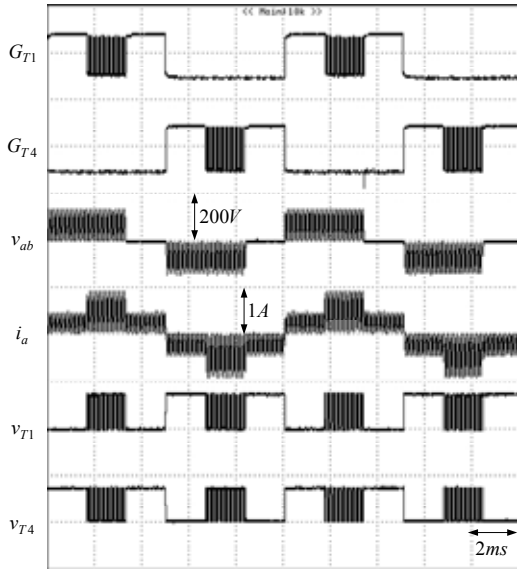

Fig. 6. Experimental waveforms for 180° SWPWM type-010_010.

References

[1] M. Gotou, and M. Ochi, "A new drive system of a brushless motor reducing power consumption and motor vibration simultaneously," in *Proc. of PEDS'99*, pp. 702-707, 1999.

[2] N. Fuji, "Small-sized motor driver IC," in *Proc. of ISPSD'04*, pp. 151-153, 2004.

[3] W. L. Hung, G. M. Link, Y. Xie, N. Vijaykrishnan, D. Dhanwada, and J. Conner, "Temperature-aware voltage islands architecting in system-on-chip design," in *Proc. of ICCD'05*, pp. 689-694.

[4] Y. S. Lai, F. S. Shyu, and Y. H. Chang, "Novel loss reduction pulse width modulation technique for brushless dc motor drives fed by MOSFET inverter", *IEEE Trans. Power Electron.,* vol. 19, no. 6, pp. 1646-1652, Nov. 2004.

[5] D. K. Kim, K. W. Lee, and B. I. Kwon, "Commutation torque ripple reduction in a position sensorless brushless dc motor drive," *IEEE Trans. Power Electron.,* vol. 21, no. 6, pp. 1762-1768, 2006.

[6] K. H. Kim, and M. J. Youn, "Performance comparison of PWM inverter and variable DC link inverter schemes for high-speed sensorless control of BLDC motor," *Electronics Letters,* vol. 38, no. 21, pp. 1294-1295, 2002.

[7] H. C. Chen, Y. C. Chang, and C. K. Huang, "Practical sensorless control for inverter-fed BDCM compressors," *IET Proc. Electric Power Applications,* vol. 1, no. 1, pp. 127-132, Jan. 2007.

[8] G. J. Su, and W. Mckeever, "Low-Cost Sensorless Control of Brushless DC Motors with Improved Speed Range," *IEEE Trans. Power Electron.,* vol. 19, no. 2, pp. 296-302, March 2004.

[9] C. C. Wang, G. N. Sung, K. W. Fang and S. L. Tseng, "A low-power sensorless inverter controller of brushless DC motors", in *Proc. of ISCAS'07*, pp. 2435-2438, 2007.

[10] P. C . Krause, O. Wasynczuk and S. D. Sudhoff, "Analysis of electric machinery and drive systems", IEEE press, Wiley-Interscience 43, no. 6, pp. 2555-2557, 2007.